American Mineralogist, Volume 58, pages 649–664, 1973

The High Temperature Crystal Chemistry of Tremolite

SHIGEHO SUENO, MARYELLEN CAMERON, J. J. PAPIKE, AND C. T. PREWITT
Department of Earth and Space Sciences,
State University of New York, Stony Brook, New York 11790

Abstract

Crystal structure parameters have been determined for tremolite $Ca_2Mg_5Si_8O_{22}(OH)_2$ at 400°C and 700°C. Anisotropic refinements in space group $C2/m$ resulted in unweighted R-factors of 0.031 and 0.044, respectively. Mean thermal expansion coefficients of the unit cell parameters decrease in the following order $\alpha_a > \alpha_b > \alpha_c$, and with increasing temperature the β_c angle decreases. Differential thermal expansion (of cation-oxygen distances) between the M-polyhedra and the T-tetrahedra [$M(4) > M(2) > M(1) > M(3) \gg T(1) = T(2)$] results in straightening of the tetrahedral chains, distortion, and tilting of the tetrahedra, and a high expansion of the A site vacancy in the a^* direction. Isotropic temperature factors for the 4-coordinated silicon atoms increase at the lowest rate and the 8-coordinated Ca atoms have the highest rate of increase. The magnitudes of the isotropic temperature factors of the Ca and Mg atoms in tremolite remain statistically identical to those in diopside over the temperature interval studied.

Introduction

Since tremolite $Ca_2Mg_5Si_8O_{22}(OH)_2$ is perhaps the least complicated of the amphiboles, we have chosen it for a study of amphibole thermal structural expansion. It has the advantages of relatively simple chemistry, no known change of space group with temperature, no cation order-disorder problems, and no problems of oxidation during the high-temperature experiments. The crystal structure of tremolite was reported by Zussman (1959) and was refined by Papike, Ross, and Clark (1969).

This is the second in a series of high-temperature amphibole studies underway in the "Petrologic Crystal Chemistry Laboratory" at Stony Brook. The first concerned the low-to-high cummingtonite transition and has been reported by Sueno, Papike, Prewitt, and Brown (1972). The present study of tremolite concerns the thermal structural expansion of tremolite with respect to expansion mechanisms and allows comparisons with diopside $CaMgSi_2O_6$ (Cameron, Sueno, Prewitt, and Papike, 1973), the pyroxene analog of tremolite. Specifically, we wish to compare: (1) the 24°C tremolite structure (Papike *et al.*, 1969) with the 400°C and 700°C tremolite structures reported here and (2) these tremolite structures with the 24°C, 400°C, 700°C, 850°C, 1000°C diopside structures (Cameron *et al.*, 1973). In addition, the data presented herein should provide valuable information for use in future studies relating thermal expansion data to more fundamental crystal properties such as atomic vibrations and chemical bonding.

Experimental

A single crystal (0.12 × 0.10 × 0.08 mm) was selected for this high-temperature study from the sample from Gouverneur, New York, mining district, used by Papike, Ross,. and Clark (1969) for the room-temperature refinement. The crystal was mounted parallel to c^* ($C2/m$) on a quartz fiber with a specially prepared high-temperature cement. The details of the crystal heater and the high-temperature cement are discussed by Brown, Sueno and Prewitt (1973). Integrated intensities were measured at 400°C (869 independent reflections) and 700°C (795 independent reflections) using a PDP-15 computer-controlled Picker four-circle diffractometer with MoKα radiation (0.7107Å) monochromatized by a graphite crystal.[1] The reflection data were collected using an $\omega - 2\theta$ scan (2°/minute) with five second background counts on each side of the peak and converted to structure factors by applying

[1] A further experiment at 850°C was attempted, but the tremolite crystal was largely converted to a polycrystalline state after 10 hours at this temperature.

Lorentz and polarization corrections, but no absorption corrections. Full matrix least-square refinement of the tremolite structure at these temperatures was carried out with the use of the RFINE program of

TABLE 2. Final Positional Parameters and Isotropic Temperature Factors for Tremolite at Several Temperatures

Atom		C2/m 24°C[b]	C2/m 400°C	C2/m 700°C	I2/m[a] 24°C	I2/m[a] 400°C	I2/m[a] 700°C
O(1)	x	0.1117(2)[c]	0.1117(2)	0.1118(3)	0.1117	0.1117	0.1118
	y	0.0860(1)	0.0862(1)	0.0863(2)	0.9140	0.9138	0.9137
	z	0.2171(3)	0.2171(5)	0.2175(6)	0.8946	0.8946	0.8943
	B	0.35(3)	1.02(4)	1.49(6)			
O(2)	x	0.1185(2)	0.1190(2)	0.1198(3)	0.1185	0.1190	0.1198
	y	0.1712(1)	0.1712(1)	0.1713(2)	0.8288	0.8288	0.8287
	z	0.7240(3)	0.7235(5)	0.7235(6)	0.3945	0.3955	0.3963
	B	0.39(3)	1.06(4)	1.52(6)			
O(3)	x	0.1096(2)	0.1104(3)	0.1106(5)	0.1096	0.1104	0.1106
	y	0	0	0	0	0	0
	z	0.7152(4)	0.7157(7)	0.7179(9)	0.3944	0.3947	0.3927
	B	0.46(4)	1.26(6)	1.79(8)			
O(4)	x	0.3654(2)	0.3658(2)	0.3662(3)	0.3654	0.3658	0.3662
	y	0.2480(1)	0.2470(1)	0.2461(2)	0.7520	0.7530	0.7539
	z	0.7933(3)	0.7951(5)	0.7958(7)	0.5721	0.5707	0.5704
	B	0.51(3)	1.42(5)	2.02(6)			
O(5)	x	0.3465(2)	0.3451(2)	0.3441(3)	0.3465	0.3451	0.3441
	y	0.1343(1)	0.1326(1)	0.1316(2)	0.8657	0.8674	0.8684
	z	0.0992(3)	0.0950(5)	0.0936(6)	0.2473	0.2501	0.2505
	B	0.46(3)	1.26(5)	1.88(6)			
O(6)	x	0.3436(2)	0.3429(2)	0.3420(3)	0.3436	0.3429	0.3420
	y	0.1185(1)	0.1192(1)	0.1194(2)	0.8815	0.8808	0.8806
	z	0.5884(3)	0.5844(5)	0.5820(6)	0.7552	0.7585	0.7600
	B	0.45(3)	1.29(5)	1.81(6)			
O(7)	x	0.3370(2)	0.3354(3)	0.3349(5)	0.3370	0.3354	0.3349
	y	0	0	0	0	0	0
	z	0.2921(5)	0.2946(7)	0.2957(10)	0.0449	0.0408	0.0392
	B	0.50(4)	1.39(7)	2.18(9)			
T(1)	x	0.2804(1)	0.2798(1)	0.2791(1)	0.2804	0.2798	0.2791
	y	0.0840(1)	0.0839(1)	0.0837(1)	0.9160	0.9161	0.9163
	z	0.2964(1)	0.2955(2)	0.2945(2)	0.9840	0.9843	0.9846
	B	0.19(1)	0.77(2)	1.07(3)			
T(2)	x	0.2887(1)	0.2882(1)	0.2880(1)	0.2887	0.2882	0.2880
	y	0.1711(1)	0.1707(1)	0.1702(1)	0.8289	0.8293	0.8298
	z	0.8042(1)	0.8032(2)	0.8027(2)	0.4845	0.485	0.4853
	B	0.19(1)	0.77(2)	1.11(3)			
M(1)	x	0	0	0	0	0	0
	y	0.0878(1)	0.0877(1)	0.0878(1)	0.9122	0.9123	0.9122
	z	0.50	0.50	0.50	0.50	0.50	0.50
	B	0.33(2)	1.02(3)	1.38(4)			
M(2)	x	0	0	0	0	0	0
	y	0.1766(1)	0.1770(1)	0.1776(1)	0.8234	0.8230	0.8224
	z	0	0	0	0	0	0
	B	0.31(2)	0.95(3)	1.38(4)			
M(3)	x	0	0	0	0	0	0
	y	0	0	0	0	0	0
	z	0	0	0	0	0	0
	B	0.33(3)	0.97(4)	1.34(5)			
M(4)	x	0	0	0	0	0	0
	y	0.2776(1)	0.2776(1)	0.2778(1)	0.7224	0.7224	0.7222
	z	0.50	0.50	0.50	0.50	0.50	0.50
	B	0.57(1)	1.53(2)	2.27(4)			

[a] Positional parameters calculated from those of the C2/m cell in order to facilitate comparison with diopside.

[b] Reported by Papike et al. (1969).

[c] Error in parentheses represents one standard deviation.

TABLE 3. Interatomic Distances in Tetrahedral Chains in Tremolite at Several Temperatures

Atom	T-O distances (Å) 24°C[a]	400°C	700°C
T(1)-O(1)	1.602(2)	1.604(2)	1.605(3)
T(1)-O(5)	1.632(2)	1.630(2)	1.626(3)
T(1)-O(6)	1.629(2)	1.628(3)	1.628(3)
T(1)-O(7)	1.616(1)	1.616(1)	1.620(2)
mean	1.620	1.620	1.620
T(2)-O(2)	1.616(2)	1.615(2)	1.612(3)
T(2)-O(4)	1.586(2)	1.586(2)	1.587(3)
T(2)-O(5)	1.653(2)	1.653(3)	1.658(3)
T(2)-O(6)	1.672(2)	1.676(2)	1.679(3)
mean	1.632	1.633	1.634
	O-O distances (Å)		
T(1) Tetrahedron	24°C[a]	400°C	700°C
O(1)-O(5)	2.681(3)	2.676(3)	2.674(4)
O(1)-O(6)	2.666(3)	2.664(3)	2.661(4)
O(1)-O(7)	2.649(2)	2.649(3)	2.657(5)
O(5)-O(6)	2.602(3)	2.603(3)	2.601(4)
O(5)-O(7)	2.638(2)	2.635(3)	2.633(4)
O(6)-O(7)	2.639(2)	2.638(3)	2.640(4)
mean	2.646	2.644	2.644
T(2) Tetrahedron			
O(2)-O(4)	2.736(2)	2.736(3)	2.735(4)
O(2)-O(5)	2.670(3)	2.667(3)	2.668(4)
O(2)-O(6)	2.665(3)	2.668(3)	2.666(4)
O(4)-O(5)	2.645(2)	2.648(3)	2.655(5)
O(4)-O(6)	2.560(2)	2.554(3)	2.553(5)
O(5)-O(6)	2.702(3)	2.704(3)	2.713(4)
mean	2.663	2.663	2.668

[a] Reported by Papike et al (1969).

L. Finger (Geophysical Laboratory). Initial positional parameters and temperature factors for the 400°C structure refinement were taken from the 24°C refinement of tremolite of Papike *et al.* (1969), and those of 700°C refinement were taken from 400°C results. Thirteen reflections were omitted from the 400°C refinement, and nineteen from the 700°C refinement, because of asymmetrical background and large ΔF ($\Delta F \geq 10$). Thirty-eight reflections in the 400°C data and 44 in the 700° data were also discarded from the refinements because they were indistinguishable from background. In the anisotropic refinement of the 400°C structure, 818 reflections (Table 1)[2] were used for the final cycle and resulted in a final unweighted R of 0.031 and

[2] Table 1 may be ordered as NAPS document #02118 from Microfiche Publications, 305 East 46th Street, New York, N. Y. 10017. Please remit in advance $1.50 for microfiche or $8.00 for photocopies. Please check the most recent issue of this journal for the current address and prices. (50 pages)

TABLE 4. Interatomic Angles (°) in Tetrahedral Chains of Tremolite at Several Temperatures

Atoms	24°C*	400°C	700°C
O(1)-T(1)-O(5)	111.9(1)	111.7(1)	111.7(2)
O(1)-T(1)-O(6)	111.1(1)	111.0(1)	110.8(2)
O(1)-T(1)-O(7)	110.7(1)	110.7(1)	111.0(2)
O(5)-T(1)-O(6)	105.8(1)	106.1(1)	106.1(2)
O(5)-T(1)-O(7)	108.5(1)	108.5(2)	108.4(2)
O(6)-T(1)-O(7)	108.7(1)	108.8(2)	108.7(2)
mean	109.4	109.5	109.5
O(2)-T(2)-O(4)	117.3(1)	117.5(1)	117.5(2)
O(2)-T(2)-O(5)	109.4(1)	109.4(1)	109.4(2)
O(2)-T(2)-O(6)	108.2(1)	108.3(1)	108.2(2)
O(4)-T(2)-O(5)	109.4(1)	109.7(1)	109.8(2)
O(4)-T(2)-O(6)	103.5(1)	103.0(1)	102.8(2)
O(5)-T(2)-O(6)	108.6(1)	108.6(1)	108.8(2)
mean	109.4	109.4	109.4
T(1)-O(5)-T(2)	136.5(1)	138.8(1)	139.2(2)
T(1)-O(6)-T(2)	138.4(1)	137.3(1)	137.6(2)
T(1)-O(7)-T(1)	139.3(2)	140.2(2)	140.2(3)
O(5)-O(6)-O(5)	167.6(1)	169.5(1)	170.4(2)
O(5)-O(7)-O(6)	166.9(2)	168.6(2)	169.4(2)
O(7)-O(7)-O(7)	65.91(7)	66.64	66.93
Δ**	0.268	0.260	0.256

*Reported by Papike et al (1969).

**$\Delta = \frac{90° - \angle[O(7)\text{-}O(7)\text{-}O(7)]}{90°}$. See Papike et al (1969) for detailed explanation.

weighted R of 0.035. In the final 700°C anisotropic structure refinement using 732 reflections (Table 1), final unweighted and weighted R's were 0.044 and 0.048, respectively. All cycles of least-square refinements were carried out using unit weights and Doyle and Turner's (1968) atomic scattering factors for neutral atoms. The results of the high-temperature structure refinements of tremolite are reported as follows: Positional parameters and isotropic temperature factors (Table 2); Interatomic distances in tetrahedral chains (Table 3); Interatomic angles in tetrahedral chains (Table 4); M–O interatomic distances (Table 5); O–O distances in M-coordination polyhedra (Table 6); Selected interatomic angles in M-coordination polyhedra (Table 7); Magnitudes and orientations of thermal ellipsoids (Table 8).

Cell parameter determinations at each temperature were made using 20 independent 2θ values which were measured just after each intensity data collection and then were included in a refinement by the PODEX2 least-squares program of Sleight.[3] Final cell parameters are listed in Table 9.

[3] Central Research Department, E. I. duPont de Nemours and Company, Wilmington, Delaware.

The expansion of cell dimensions and interatomic distances with increasing temperature are described on the basis of the "mean thermal expansion coefficient" (MTEC) throughout this paper. The MTEC was calculated using the following equation:

$$\alpha_X = \frac{1}{X_{24}} \cdot \frac{X_T - X_{24}}{T - 24} \,°C^{-1}$$

where X_{24} is the value of a particular parameter at room temperature and X_T is the value at some higher temperature. Rate of increase, rather than α_X, has been used occasionally to describe certain figures in the paper since the rate of increase (*i.e.*, the slope) is directly observable on these diagrams.

Amphibole Structure

The $C2/m$ amphibole structure is characterized by chains of hexagonal rings running parallel to c that consist of two non-equivalent tetrahedra $T(1)$ and $T(2)$. The chains form layers parallel to (100) and

TABLE 5. M–O Interatomic Distances (Å) in Tremolite at Several Temperatures

Atoms	Distance 24°C [a]	400°C	700°C	MTEC[b] (x 10^5)
M(1)-O(1)	2.064(2)	2.068(2)	2.071(3)	0.502
M(1)-O(2)	2.078(2)	2.089(2)	2.100(3)	1.560
M(1)-O(3)	2.083(2)	2.094(2)	2.110(4)	1.898
mean for 6	2.075	2.084	2.094	1.345
M(2)-O(1)	2.133(2)	2.145(2)	2.161(3)	1.927
M(2)-O(2)	2.083(2)	2.094(2)	2.105(3)	1.597
M(2)-O(4)	2.014(2)	2.024(2)	2.033(4)	1.464
mean for 6	2.077	2.088	2.100	1.627
M(3)-O(1)	2.070(2)	2.082(2)	2.093(3)	1.640
M(3)-O(3)	2.057(3)	2.065(3)	2.061(4)	0.317
mean for 6	2.066	2.076	2.082	1.152
M(4)-O(2)	2.397(2)	2.406(2)	2.421(3)	1.463
M(4)-O(4)	2.321(2)	2.328(2)	2.331(3)	0.642
M(4)-O(6)	2.539(2)	2.538(2)	2.544(3)	0.275
M(4)-O(5)	2.767(2)	2.814(2)	2.841(4)	3.993
mean for 6	2.419	2.424	2.435	0.961
mean for 8	2.506	2.521	2.534	1.651
M(1)-M(1)	3.169(2)	3.178(3)	3.196(4)	1.240
M(1)-M(2)	3.086(2)	3.099(1)	3.111(2)	1.197
M(1)-M(3)	3.077(1)	3.084(1)	3.093(1)	0.763
M(1)-M(4)	3.423(2)	3.440(2)	3.455(3)	1.380
M(2)-M(3)	3.187(2)	3.208(1)	3.230(2)	1.987
M(2)-M(4)	3.204(1)	3.210(1)	3.215(1)	0.508

[a] Reported by Papike et al (1969).

[b] MTEC: Mean thermal expansion coefficient. See text of paper for explanation.

TABLE 6. O–O Interatomic Distances (Å) in *M*-Coordination Polyhedra in Tremolite at Several Temperatures

	24°C	400°C	700°C	MTEC[a] (x 10^5)
M(1) site				
$O(1^u)$-$O(2^u)$[b]	3.070(3)	3.073(3)	3.077(4)	0.334
$O(1^u)$-$O(3^u)$	3.056(3)	3.066(4)	3.083(5)	1.290
O(2)-O(3)	3.090(2)	3.103(2)	3.117(3)	1.286
$O(1^u)$-$O(2^d)$	2.815(2)	2.829(3)	2.846(4)	1.618
$O(1^u)$-$O(3^d)$	2.765(3)	2.785(3)	2.794(5)	1.566
O(2)-O(2)	2.867(3)	2.881(4)	2.903(6)	1.887
O(3)-O(3)	2.704(3)	2.727(6)	2.756(10)	2.824
mean	2.908	2.923	2.940	1.618
M(2) site				
$O(1^u)$-$O(2^u)$	3.037(3)	3.045(3)	3.057(4)	0.961
$O(2^u)$-$O(4^d)$	2.982(3)	3.008(3)	3.031(4)	2.428
O(4)-O(4)	2.970(3)	2.968(4)	2.972(7)	0.088
O(1)-O(4)	3.006(2)	3.032(3)	3.057(4)	2.503
$O(1^u)$-$O(2^d)$	2.815(2)	2.829(3)	2.846(4)	1.618
$O(2^u)$-$O(4^u)$	2.904(3)	2.915(3)	2.930(4)	1.311
$O(1^u)$-$O(1^d)$	2.741(3)	2.752(4)	2.767(6)	1.389
mean	2.922	2.935	2.951	1.455
M(3) site				
$O(1^u)$-$O(1^u)$	3.104(2)	3.125(4)	3.141(6)	1.765
$O(1^u)$-$O(3^u)$	3.064(3)	3.073(4)	3.075(5)	0.536
$O(1^u)$-$O(1^d)$	2.741(3)	2.752(4)	2.767(6)	1.389
$O(1^u)$-$O(3^d)$	2.765(3)	2.785(3)	2.794(5)	1.566
mean	2.892	2.906	2.916	1.230
M(4) site				
$O(2^u)$-$O(4^u)$	3.133(3)	3.153(3)	3.167(4)	1.609
O(2)-O(6)[c]	4.192	4.185	4.191	-0.053
O(4)-O(6)	2.560(2)	2.554(3)	2.553(5)	-0.415
O(6)-O(6)	3.426(3)	3.433(4)	3.449(6)	0.975
$O(2^u)$-$O(4^d)$	2.982(3)	3.008(3)	3.031(4)	2.428
O(2)-O(2)	2.867(3)	2.881(4)	2.903(6)	1.887

[a] MTEC: Mean thermal expansion coefficient. See text of paper for explanation.

[b] The superscript notation u = up, d = down refers to oxygen x values greater (u) or less (d) than the x of M.

[c] Calculated by hand.

are bound together by strips of cations which occupy four non-equivalent sites: the octahedral $M(1)$, $M(2)$ and $M(3)$ sites and the 8-coordinated $M(4)$ site. In tremolite, the $M(4)$ site is occupied by Ca, the smaller octahedral sites by Mg, and both tetrahedral sites by Si. The A site, which is located between the tetrahedral chains, is vacant in tremolite. A projection of the tremolite structure down a^* is shown in Figure 1.

Amphiboles are most commonly reported in space group $C2/m$, but in order to facilitate comparison of the tremolite structure with that of diopside, we have recalculated selected parameters of tremolite in the $I2/m$ space group. The transformation from the C-centered to the I-centered cell was made using the matrix $101/0\bar{1}0/00\bar{1}$.

Thermal Expansion of Unit Cell Parameters

Unit cell parameters of tremolite for both the C-centered and I-centered unit cells (Table 9) vary linearly with increasing temperature, (Figure 2a-e).

TABLE 7. Selected Interatomic Angles (°) in the $M(1)$, $M(2)$, $M(3)$, and $M(4)$ Sites of Tremolite at Several Temperatures

Atoms	24°C[a]	400°C	700°C
$O(1^u)$-M(1)-$O(2^u)$[b]	95.68(7)	95.32(9)	95.06(12)
$O(1^u)$-M(1)-$O(2^d)$	85.63(7)	85.76(9)	86.03(12)
$O(1^u)$-M(1)-$O(3^u)$	94.96(9)	94.90(11)	95.01(15)
$O(1^u)$-M(1)-$O(3^d)$	83.66(9)	83.97(11)	83.85(15)
O(2)-M(1)-O(2)	87.23(8)	87.19(12)	87.43(19)
O(3)-M(1)-O(3)	80.96(8)	81.27(14)	81.55(21)
O(2)-M(1)-O(3)	95.91(7)	95.78(9)	95.53(13)
O(1)-M(2)-O(1)	79.95(7)	79.82(12)	79.65(18)
$O(1^u)$-M(2)-$O(2^u)$	92.11(7)	91.84(9)	91.53(12)
$O(1^u)$-M(2)-$O(2^d)$	83.74(7)	83.72(8)	83.68(12)
O(1)-M(2)-O(4)	92.83(6)	93.26(8)	93.55(13)
$O(2^u)$-M(2)-$O(4^u)$	90.25(8)	90.11(9)	90.10(13)
$O(2^u)$-M(2)-$O(4^d)$	93.40(7)	93.82(9)	94.15(13)
O(4)-M(2)-O(4)	95.00(8)	94.31(14)	93.91(22)
$O(1^u)$-M(3)-$O(1^u)$	97.09(6)	97.26(11)	97.24(17)
$O(1^u)$-M(3)-$O(1^d)$	82.91(7)	82.74(11)	82.76(17)
$O(1^u)$-M(3)-$O(3^u)$	95.86(6)	95.64(8)	95.48(12)
$O(1^u)$-M(3)-$O(3^d)$	84.14(6)	84.36(8)	84.52(12)
O(2)-M(4)-O(6)	116.17(6)	115.62(6)	115.13(10)
$O(2^u)$-M(4)-$O(4^u)$	83.19(6)	83.48(8)	83.57(11)
$O(2^u)$-M(4)-$O(4^d)$	78.42(6)	78.87(7)	79.25(11)
O(2)-M(4)-O(2)	73.46(6)	73.55(10)	73.68(15)
$O(4^u)$-M(4)-$O(6^u)$	66.53(5)	63.14(7)	62.98(10)
$O(4^u)$-M(4)-$O(6^d)$	137.90(5)	137.19(8)	136.77(12)
O(6)-M(4)-O(6)	84.89(7)	85.12(10)	85.37(15)
O(4)-M(4)-O(4)	157.03(6)	157.94(11)	158.49(17)

[a] Reported by Papike et al (1969).

[b] The superscript notation u = up, d = down refers to oxygen x values greater (u) or less (d) than the x of M.

The a dimension exhibits the largest mean thermal expansion coefficient and c the smallest. By contrast, in diopside the b cell dimension has the largest mean thermal expansion coefficient and c the smallest. The differences in thermal expansion behavior may be related to the large, vacant A site in tremolite. The β_C angle for the C-centered cell decreases linearly with temperature whereas β_I (which corresponds to β_c for $C2/c$ pyroxenes) increases, as is observed in the calcic pyroxenes diopside and hedenbergite.

Polyhedral Expansions

The changes in mean Si–O interatomic distances with increasing temperature (Table 3) are statistically insignificant over the temperature interval stud-

TABLE 8. Magnitude and Orientation of the Principal Axes of the Thermal Ellipsoids in Tremolite at Several Temperatures

Atom	Ellipsoid axis	24°C[a] rms amplitude Å	24°C[a] Angles, degrees with respect to a	b	c	400°C rms amplitude Å	400°C Angles, degrees with respect to a	b	c	700°C rms amplitude Å	700°C Angles, degrees with respect to a	b	c
O(1)	r_1	0.061(5)[b]	18(25)	108(23)	104(127)	0.104(4)	168(25)	100(33)	69(13)	0.125(6)	160(19)	98(50)	58(13)
	r_2	0.067(4)	94(34)	104(43)	157(38)	0.109(4)	82(34)	167(24)	102(15)	0.130(6)	84(55)	171(50)	98(33)
	r_3	0.072(4)	107(18)	157(33)	71(43)	0.127(6)	82(10)	99(13)	24(11)	0.155(6)	71(9)	95(10)	34(9)
O(2)	r_1	0.052(6)	177(8)	89(9)	73(8)	0.103(4)	6(12)	84(10)	102(11)	0.121(6)	150(10)	75(15)	51(8)
	r_2	0.076(3)	89(10)	8(73)	98(70)	0.118(5)	84(12)	146(32)	124(32)	0.139(6)	74(16)	16(15)	96(17)
	r_3	0.078(4)	88(9)	82(74)	19(34)	0.126(6)	89(10)	123(33)	36(32)	0.154(5)	65(9)	95(17)	40(8)
O(3)	r_1	0.066(8)	166(15)	90	62(15)	0.120(5)	90	0	90	0.130(6)	90	0	90
	r_2	0.074(6)	90	0	90	0.122(9)	46(22)	90	151(22)	0.130(6)	48(7)	90	152(7)
	r_3	0.084(5)	76(15)	90	28(15)	0.137(5)	44(22)	90	61(22)	0.184(7)	42(7)	90	62(7)
O(4)	r_1	0.054(5)	62(7)	29(5)	90(8)	0.094(5)	122(3)	148(4)	79(6)	0.109(8)	117(4)	153(4)	83(3)
	r_2	0.079(6)	49(9)	105(9)	148(8)	0.134(6)	61(7)	111(6)	154(6)	0.153(6)	48(6)	110(6)	144(5)
	r_3	0.098(3)	54(7)	115(4)	58(8)	0.164(4)	46(5)	113(3)	66(7)	0.203(5)	53(4)	107(3)	55(5)
O(5)	r_1	0.054(8)	135(14)	118(5)	47(12)	0.100(7)	110(9)	119(5)	31(5)	0.114(7)	124(6)	122(5)	40(4)
	r_2	0.068(4)	130(14)	82(8)	124(12)	0.124(4)	158(8)	88(8)	98(8)	0.159(6)	145(6)	63(9)	97(8)
	r_3	0.099(3)	106(4)	29(4)	63(4)	0.151(4)	99(6)	30(5)	61(5)	0.182(5)	83(9)	44(7)	51(4)
O(6)	r_1	0.060(6)	173(23)	92(6)	69(24)	0.101(7)	112(7)	59(5)	33(6)	0.123(7)	115(11)	54(5)	39(6)
	r_2	0.069(4)	97(24)	90(8)	159(24)	0.130(4)	155(7)	90(10)	101(7)	0.148(6)	152(10)	94(9)	104(10)
	r_3	0.092(3)	88(5)	178(5)	91(16)	0.147(4)	102(9)	149(5)	60(6)	0.179(6)	103(7)	144(5)	55(5)
O(7)	r_1	0.053(6)	90	0	90	0.094(6)	90	0	90	0.087(13)	90	0	90
	r_2	0.056(9)	3(5)	90	107(5)	0.124(5)	7(6)	90	112(6)	0.161(8)	2(5)	90	107(5)
	r_3	0.111(5)	87(5)	90	17(5)	0.169(7)	83(6)	90	22(6)	0.223(7)	88(5)	90	17(5)
T(1)	r_1	0.036(4)	143(6)	123(6)	64(6)	0.089(2)	71(7)	19(7)	92(7)	0.093(3)	115(7)	154(8)	77(5)
	r_2	0.052(2)	126(8)	37(12)	88(20)	0.099(2)	27(10)	107(8)	125(12)	0.108(3)	37(6)	116(8)	127(4)
	r_3	0.056(2)	82(15)	77(19)	26(6)	0.109(3)	71(11)	99(6)	35(12)	0.142(2)	65(3)	94(2)	40(3)
T(2)	r_1	0.031(4)	147(4)	119(4)	64(6)	0.086(2)	137(5)	131(6)	71(8)	0.093(3)	139(4)	126(6)	61(4)
	r_2	0.051(2)	108(8)	86(12)	147(9)	0.098(3)	67(10)	126(7)	142(8)	0.113(3)	65(5)	141(6)	123(4)
	r_3	0.058(2)	117(5)	29(5)	72(12)	0.110(2)	56(6)	118(6)	58(9)	0.144(2)	60(3)	102(3)	47(3)
M(1)	r_1	0.060(3)	90	0	90	0.105(3)	90	0	90	0.112(5)	136(4)	90	32(4)
	r_2	0.063(4)	22(19)	90	127(19)	0.108(4)	40(10)	90	145(10)	0.122(4)	90	180	90
	r_3	0.070(3)	68(19)	90	37(19)	0.126(3)	50(10)	90	55(10)	0.158(4)	46(4)	90	58(4)
M(2)	r_1	0.055(5)	162(9)	90	58(9)	0.099(5)	137(7)	90	32(7)	0.115(4)	142(4)	90	38(4)
	r_2	0.057(3)	90	0	90	0.103(3)	90	180	90	0.118(4)	90	180	90
	r_3	0.072(3)	72(9)	90	32(9)	0.125(3)	47(7)	90	58(7)	0.159(4)	52(4)	90	52(4)
M(3)	r_1	0.048(5)	90	0	90	0.100(4)	90	0	90	0.109(7)	122(5)	90	17(5)
	r_2	0.068(5)	178(40)	90	77(40)	0.112(6)	48(25)	90	153(25)	0.118(6)	90	180	90
	r_3	0.074(4)	92(40)	90	13(40)	0.121(4)	42(25)	90	63(25)	0.158(5)	32(5)	90	73(5)
M(4)	r_1	0.048(4)	143(1)	90	39(1)	0.104(3)	144(1)	90	40(1)	0.120(3)	145(10)	90	41(10)
	r_2	0.077(1)	90	0	90	0.121(2)	90	180	90	0.137(3)	90	180	90
	r_3	0.105(1)	53(1)	90	51(1)	0.181(2)	54(1)	90	50(1)	0.231(2)	55(10)	90	49(10)

[a] Reported by Papike, Ross and Clark (1969).

[b] Error in parentheses represents one standard deviation.

TABLE 9. Unit Cell Parameters of Tremolite at Several Temperatures

	C2/m cell				I2/m cell[c]			
	24°C[a]	400°C	700°C	MTEC[b] (x 10^5)	24°C	400°C	700°C	MTEC (x 10^5)
a(Å)	9.818(5)[d]	9.860(1)	9.898(2)	1.202	9.901	9.947	9.992	1.355
b(Å)	18.047(8)	18.118(3)	18.190(3)	1.167	18.047	18.118	18.190	1.167
c(Å)	5.275(3)	5.285(1)	5.296(1)	0.583	5.275	5.285	5.296	0.583
β(°)	104.65(5)	104.57(1)	104.46(1)	-0.266	106.38	106.38	106.42	0.052
V(Å^3)	904.2(6)	913.8(2)	923.4(2)	3.131	904.2	913.8	923.4	3.131
a sinβ(Å)	9.499	9.543	9.584	1.320	9.499	9.543	9.584	1.320

[a]Reported by Papike, Ross and Clark (1969).
[b]MTEC: Mean thermal expansion coefficient. See text of paper for explanation.
[c]Cell parameters calculated from those of the C2/m cell in order to facilitate comparison with diopside. Transformation matrix is given in text of paper.
[d]Errors in parentheses represent one standard deviation.

ied. The mean $T(1)$–O distances show no change and the mean $T(2)$–O distance increases 0.002Å, approximately one standard deviation. Changes in tetrahedral O–O distances (Table 3) and angles (Table 4) are usually within three standard deviations. The change in volume of the two tetrahedra with increasing temperature is also negligible (Table 10).

The $M(1)$, $M(2)$, $M(3)$ and $M(4)$ polyhedra exhibit much larger thermal expansions (Table 5) than do the silicate tetrahedra. The variation of mean M–O bonds and polyhedral volumes are shown in Figures 3 and 4, respectively. Mean thermal expansion coefficients for the mean M–O bonds (Table 5) decrease in the order $M(4) > M(2) > M(1) > M(3)$. Polyhedral volumes (Table 10) vary similarly, with the exception of $M(4)$ which lies between $M(2)$ and $M(1)$. Larger values for the $M(2)$ site relative to $M(1)$ and $M(3)$ may be related to its position near the edge of the octahedral strip in the amphibole structure. Comparison of mean thermal expansion coefficients for both mean M–O bonds and polyhedral volumes for comparable sites in tremolite and diopside reveal some similarity, as shown below

Mean Thermal Expansion Coefficients

Tremolite		Diopside	
Mean M–O distances			
Bond	$\alpha_{\text{mean M–O}}$	Bond	$\alpha_{\text{mean M–O}}$
$M(4)$–O	1.65×10^{-5}/°C	$M(2)$–O	1.64×10^{-5}/°C
$M_{\text{avg. oct.}}$	1.38×10^{-5}/°C	$M(1)$–O	1.44×10^{-5}/°C
Polyhedral volumes			
Polyhedron	$\alpha_{\text{poly. vol.}}$	Polyhedron	$\alpha_{\text{poly. vol.}}$
$T_{\text{avg. tet.}}$	0.041×10^{-5}/°C	T	0.057×10^{-5}/°C
$M(4)$	4.50×10^{-5}/°C	$M(2)$	4.42×10^{-5}/°C
$M_{\text{avg. oct.}}$	4.26×10^{-5}/°C	$M(1)$	4.26×10^{-5}/°C

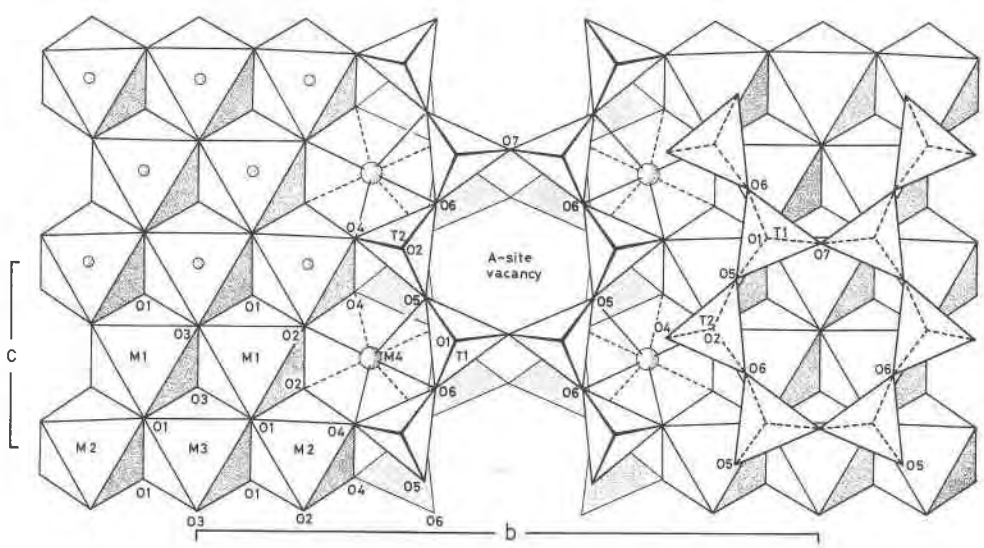

FIG. 1. Diagram of the tremolite structure at 24°C viewed along a^*.

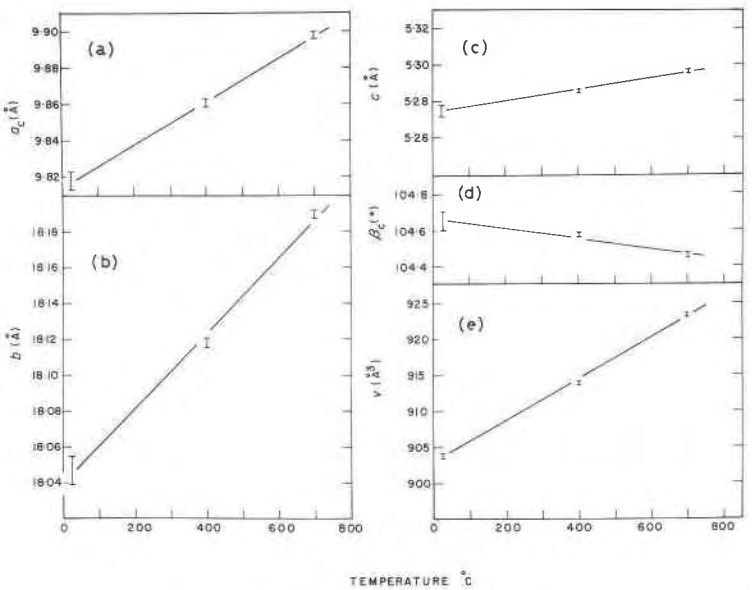

FIG. 2. Variation with increasing temperature of the unit cell parameters in tremolite for the $C2/m$ space group. Error bars represent ± 1 standard deviation.

Interestingly, if the $M(4)$ cation in tremolite is considered as being 6-coordinated, then the mean $M(4)$–O distance exhibits a smaller mean thermal expansion coefficient than the mean M–O bonds in any of the three octahedra, whereas 6-coordinated $M(4)$ polyhedral volume exhibits a larger mean thermal expansion coefficient than any of the octahedra (Table 10).

The variations of individual M–O bonds with increasing temperature are shown in Figure 5a-d. In the $M(1)$ and $M(3)$ octahedra, the $M(1)$–O(1) and $M(3)$–O(3) bonds, which lie in a plane at or near 90° to the b axis, exhibit the smallest mean thermal expansion coefficients of any of the octahedral bonds. The rate of increase of the $M(4)$–O(5) bond (Fig. 5d) is significantly greater than that of the $M(4)$–O bonds, and may reflect both a straightening of the O(5)–O(6)–O(5) tetrahedral chain angle and the relative displacement of the tetrahedral chains. The $M(4)$–O(4) bond, which has large bond length components in both the a and c crystallographic directions, has a relatively small rate of expansion.

The changes in volume and shape of the vacant A site with increasing temperature in tremolite were examined (Tables 10, 11, and Figure 6). The mean thermal expansion coefficient of the volume of a 12-coordinated A site (Table 11) is smaller than that observed for any of the M-coordination polyhedra;

TABLE 10. Volumes (Å³) of Tremolite and Diopside Polyhedra at Several Temperatures

	Tremolite			
Polyhedra	24°C	400°C	700°C	MTEC[a] (x 10^5)
M(1)	11.723	11.885	12.066	4.308
M(2)	11.828	12.011	12.218	4.855
M(3)	11.532	11.705	11.813	3.623
M(4) 6-coordinated	12.536	12.787	13.026	5.774
M(4) 8-coordinated	26.111	26.530	26.906	4.498
T(1)	2.182	2.178	2.179	-0.100
T(2)	2.219	2.217	2.222	0.182
A vacancy 10-coordinated	47.116	47.996	48.708	5.003
A vacancy 12-coordinated	57.116	57.641	58.200	2.805
	Diopside[b]			
Polyhedra	24°C	400°C	700°C	MTEC[a] (x 10^5)
M(1)	11.848	12.047	12.206	4.258
M(2)	25.706	26.193	26.576	4.421
T	2.221	2.229	2.228	0.057

[a]MTEC: Mean thermal expansion coefficient. See text of paper for explanation.

[b]Reported by Cameron et al (1973).

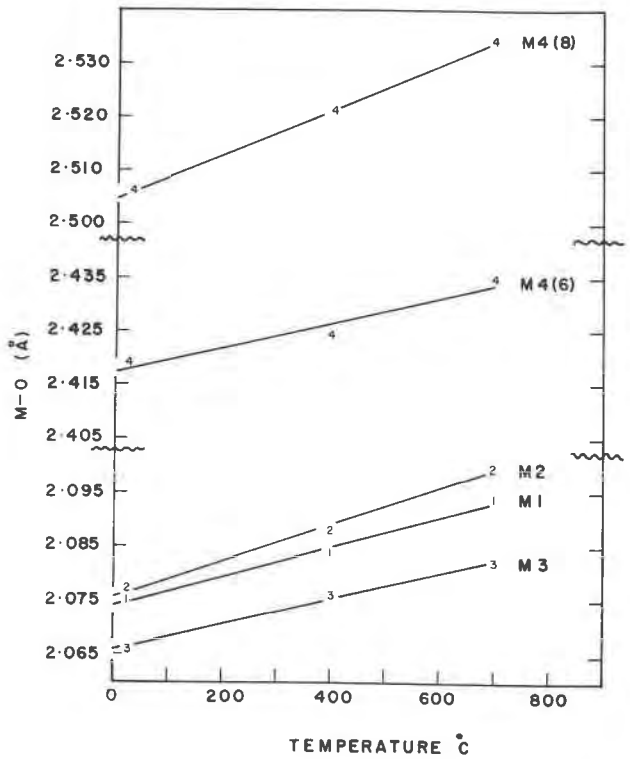

FIG. 3. Variation of mean M–O interatomic distances with increasing temperature. The numbers in parentheses represent the number of coordinating oxygen atoms which have been used for calculation of the mean $M(4)$–O distances. The small numbers plotted on the diagram indicate the observed mean M–O distances at 24°C, 400°C and 700°C.

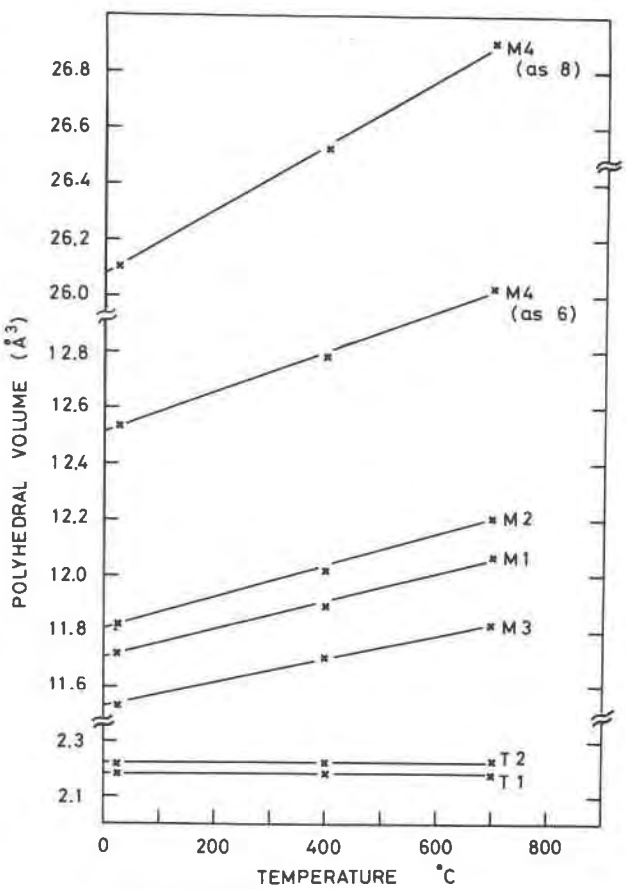

FIG. 4. Variation of polyhedral volumes in tremolite with increasing temperature.

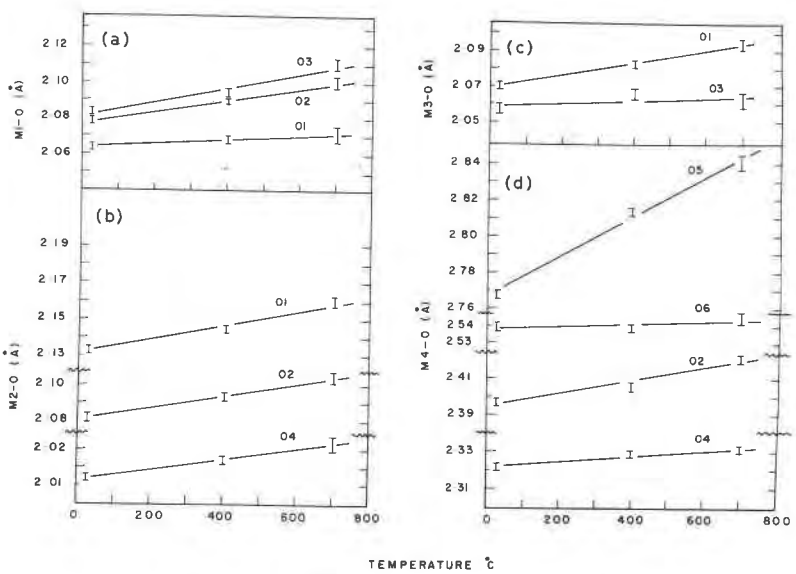

FIG. 5. Variation of individual M–O interatomic distances in tremolite with increasing temperature: (a) in the $M(1)$ octahedron; (b) in the $M(2)$ octahedron; (c) in the $M(3)$ octahedron; (d) in the $M(4)$ polyhedron. Error bars represent ± 1 standard deviation.

however, since the site is vacant, it may well behave passively during thermal expansion. With increasing temperature, the *A* site does expand considerably in the *a* or *a** direction.

Differential Polyhedral Expansion

The small expansion of the Si–O bond in tremolite relative to the other *M*–O bonds has been reported in other chain silicates (Smyth and Burnham, 1972; Smyth, 1971; Brown *et al,* 1972; Sueno *et al,* 1972; and Cameron *et al,* 1973) and is undoubtedly a result of the greater strength of the Si–O bond relative to the *M*–O bonds. Because of this differential polyhedral expansion, there is a potential structural misfit between the tetrahedral chains and the octahedral layers to which they are connected. The necessary accommodation is achieved principally by straightening of the tetrahedral chains and tilting of the tetrahedra out of the *bc* plane (Papike, Sueno, Cameron, and Prewitt, in preparation). During the thermal expansion of tremolite, the O(5)–O(6)–O(5) angle increases from 167.6° ± 0.1 at 24°C to 170.4° ± 0.2 at 700°C. Over this same temperature interval, the *T*(2) tetrahedra tilts additionally about 0.7°, but the *T*(1) tetrahedra negligibly, about an axis approximately parallel to *c*. Rotation about an axis approximately parallel to *b* decreases the tilt of the *T*(1) and *T*(2) tetrahedra by about 0.3°, causing the O(5)–O(6) atoms to become more coplanar.[4] The increase in tilt of the *T*(2) tetrahedra about an axis approximately parallel to *c* is similar in magnitude to the increase in the out-of-plane tilting of tetrahedra observed in the pyroxenes (Cameron *et al,* 1973).

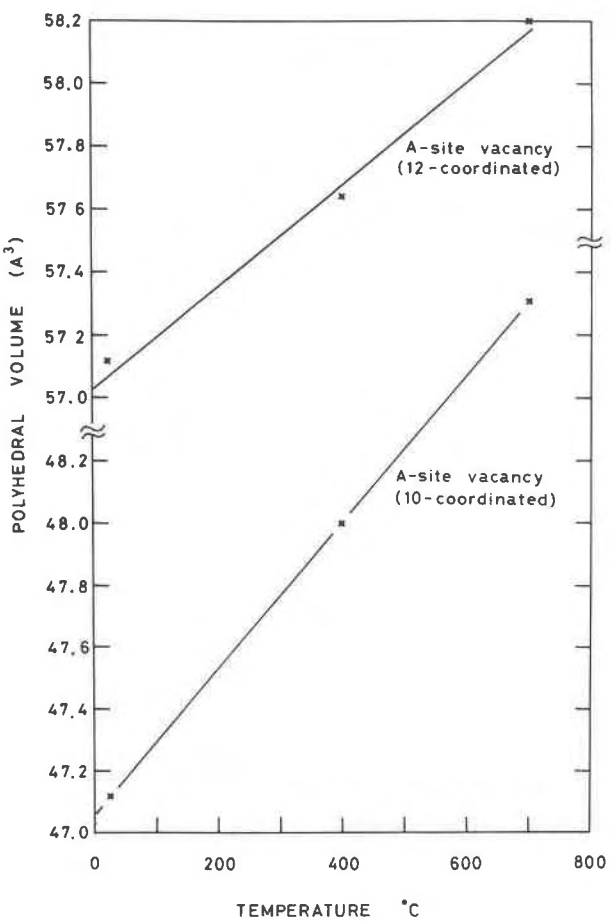

FIG. 6. Variation with increasing temperature of the volume of the vacant *A* site polyhedron in tremolite.

TABLE 11. Interatomic Distances (Å) in the *A* Site of Tremolite at Several Temperatures

Atoms	Bond multiplicity	Temperature 24°C	400°C	700°C	MTEC[a] (x 10^5)
A-O(5)[b]	4	2.970	2.957	2.956	-0.715
A-O(6)	4	3.156	3.190	3.215	1.303
A-O(7)	2	2.486	2.516	2.530	2.640
A-O(7)	2	3.672	3.673	3.680	0.311
mean for 10		2.948	2.962	2.974	1.302
mean for 12		3.068	3.081	3.092	1.157

[a] MTEC: Mean thermal expansion coefficient. See text of paper for explanation.

[b] A-O distances calculated for atom assumed to be at 1/2, 0, 0.

Differential polyhedral expansion can also be used to explain the relatively large expansion of the *A* site of tremolite in the *a** direction. During thermal expansion, the O(1) and O(2) atoms, which co-

[4] In our notation, the change in tilt angle around *c* would be +0.7° whereas that around *b* would be −0.3°. The magnitude of tilting (or rotation) about an axis approximately parallel to *c* for each tetrahedron was determined in the following manner. For both the 24° and the 700° tremolite structures, a line was defined between the O(7) atom and the midpoint of the O(5)–O(6) tetrahedral edge for the *T*(1) tetrahedra, and between O(4) and the midpoint of the O(5)–O(6) edge for the *T*(2) tetrahedra. The angles that these lines make with the *bc* plane are largely a result of rotation about *c*. The magnitude of rotation about an axis approximately parallel to *b* was determined by calculating the angles between the O(5)–O(6) vector and the *bc* plane for the 24° and 700° structures. At 700° the rotation angle is smaller, indicating that the O(5) and O(6) atoms are becoming more coplanar.

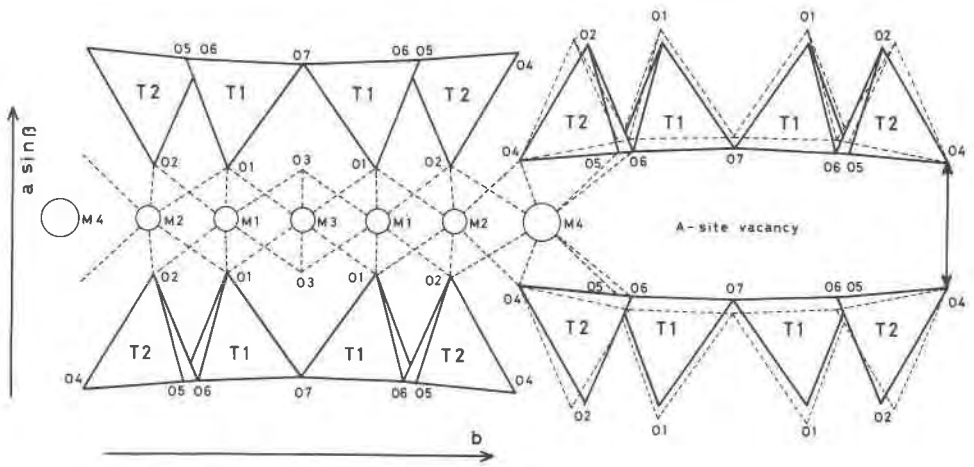

FIG. 7. Diagram of tremolite structure at 24°C viewed along *c*. The broken lines associated with the tetrahedral chains show their movement with increasing temperature (the movement is highly exaggerated in this diagram).

ordinate both the octahedral and tetrahedral cations, are displaced laterally along the *b* axis as a result of the large thermal expansions of the octahedra. Because the Si–O bonds are relatively strong, it may be easier for the entire tetrahedra to tilt about an axis parallel to *c* rather than distort to accommodate the shift of the apical oxygens. Tilting of the $T(2)$ tetrahedra (Fig. 7) moves the bridging O(5) and O(6) atoms farther from the *bc* plane, thus increasing the *A* site dimension in the a^* direction. During thermal expansion, the projection of the O(4)–O(4) edge of the $M(2)$ octahedron onto the *ab* plane changes very little.

Thermal Parameters

Isotropic Temperature Factors

Equivalent isotropic temperature factors for the Si, Mg, and Ca atoms in both tremolite and diopside are shown in Figure 8. The rate of increase of the 4-coordinated Si atom in tremolite is lower than that of 6-coordinated Mg and the 8-coordinated Ca has the highest rate of increase. This is in agreement with what has been generally observed in end-member pyrozenes (Cameron *et al,* 1973). The Mg atoms in the $M(1)$, $M(2)$, and $M(3)$ octahedra in tremolite maintain statistically identical values with increasing temperature, as do the silicon atoms in $T(1)$ and $T(2)$. Figure 8 reveals that the rate of increase for the Ca and Mg atoms in tremolite and diopside are remarkably similar.

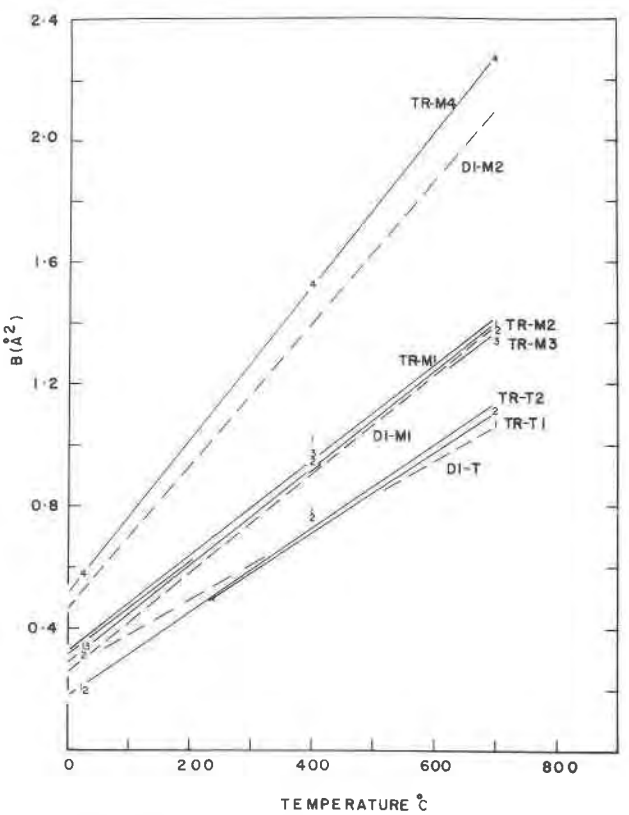

FIG. 8. Variation with increasing temperature of equivalent isotropic temperature factors of cations in tremolite (solid lines), and in diopside (broken lines). The small numbers plotted on the diagram indicate the values obtained during refinements of the structures. Abbreviations: TR = tremolite, DI = diopside.

The equivalent isotropic temperature factors of the oxygen atoms in tremolite also show a relationship with coordination number. $B(Å^2)$ for the two-coordinated O(7) atom shows the highest rate of increase (Fig. 9 and Table 12) whereas the tetrahedrally coordinated apical oxygens O(1) and O(2) exhibit the lowest rate of increase. The coordination of the O(1) atom in diopside is similar to that of the O(1) and O(2) atoms in tremolite (all are coordinated by three metal atoms and one Si atom) and the coordination of O(2) in diopside is similar to that of O(4) in tremolite (both are coordinated by one Si, one Mg, and one Ca). The similarities are reflected in the close correspondence of related temperature factors. The rate of increase of $B(Å^2)$ of the hydroxyl [occupying the O(3) site] is slightly lower but, in general, similar to that of the other 3-coordinated oxygen atoms in tremolite. The O(3) atom in diopside, coordinated by two Ca and two Si atoms in distorted tetrahedral arrangement, has a coordination for which there is no corresponding arrangement in tremolite. The higher values for the rate of increase of this tetrahedrally coordinated oxygen relative to that of O(1) may be related to the two relatively longer Ca–O bonds.

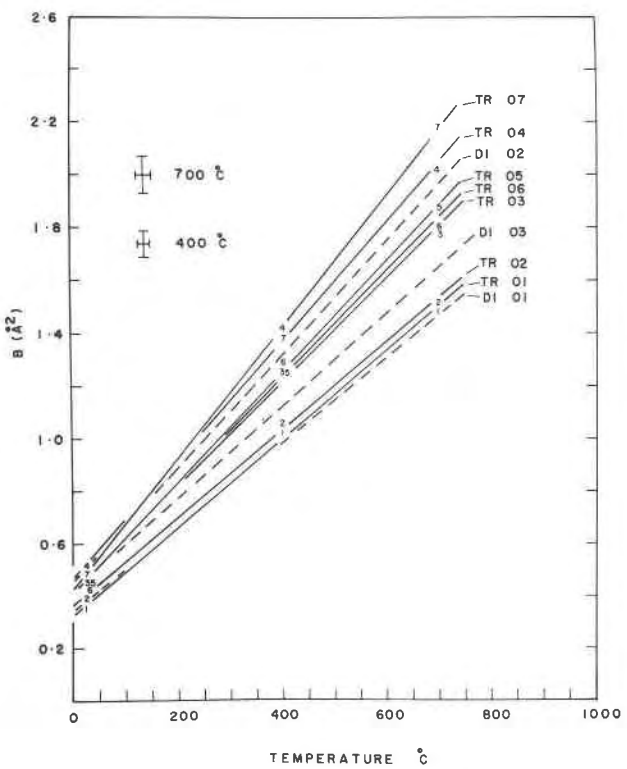

FIG. 9. Variation of equivalent isotropic temperature factors of oxygen atoms in tremolite (solid lines) and diopside (broken lines) with increasing temperature. The errors for temperature factors ($\pm 1\sigma$) and temperature are indicated in the upper left of the diagram. (The small numbers and abbreviations are the same as those in Figure 8.)

TABLE 12. Rate of Increase ($Å^2/°C \times 10^3$) of Isotropic Temperature Factors in Tremolite and Diopside

Tremolite			
Atom	Rate of increase[a]	Atom	Rate of increase[a]
O(1)	1.69	M(1)	1.56
O(2)	1.68	M(2)	1.59
O(3)	1.97	M(3)	1.50
O(4)	2.24	M(4)	2.52
O(5)	2.10	T(1)	1.31
O(6)	2.02	T(2)	1.37
O(7)	2.48		

Diopside[b]			
Atom	Rate of increase[a]	Atom	Rate of increase[a]
O(1)	1.62	M(1)	1.62
O(2)	2.16	M(2)	2.33
O(3)	1.76	T	1.14

[a] Rate of increase $(\frac{dB}{dT}) = \frac{B_T - B_{24}}{T - 24}$

[b] Reported by Cameron et al (1973).

Thermal Ellipsoids

The O(7) atom is the only oxygen that has a highly anisotropic thermal ellipsoid. It is located on a mirror plane; and, as a result, one axis of the thermal ellipsoid must be at right angles to the mirror, and the remaining two axes must lie within the mirror plane. The longest axis of the O(7) thermal ellipsoid is almost parallel to the *c* crystallographic axis, and the shortest ellipsoid axis is parallel to the *b* crystallographic axis. The orientation of the short axis is reasonable since the two silicon atoms which coordinate O(7) lie on a line parallel to the *b* axis.

The *M*(1), *M*(2), *M*(3) and *M*(4) atoms lie on 2-fold rotation axes; consequently, one thermal ellipsoid axis must lie parallel to the 2-fold axis and the remaining two ellipsoid axes must lie in a plane at right angles to the first. In general, the longest ellipsoid axis for all four *M* cations lies at about 50° from the a_c axis and 50° from the c_c axis. For atoms *M*(1), *M*(2), *M*(3), and *M*(4), these longest axes are almost normal to the following bonds: O(1)–*M*(1)–O(1); O(2)–*M*(2)–O(2); O(3)–*M*(3)–

O(3); and O(4)–M(4)–O(4). The M(4) atom is the only cation that is highly anisotropic, and a projection onto the *ac* plane of its thermal ellipsoid is shown in Figure 10. The ellipsoid is prolate and its relative magnitude at 24°C and 700°C is shown. A similar shape and orientation has been observed for the Ca atom in the M(2) site in diopside (Cameron *et al,* 1973).

In a study of cummingtonite (Sueno *et al,* 1972; and unpublished data), it was found that with increasing temperature the M(4) cation moves along the 2-fold axis toward the O(5)–O(6) side of the M(4) polyhedron. This same phenomenon was observed in tremolite with increasing temperature. Recent investigations of room-temperature amphiboles and pyroxene structures (Papike *et al,* 1969; Takeda, 1972) show that the position of the cation in the M(4) site in amphibole and the M(2) site in pyroxene depends in large part upon the size of the cation. In amphiboles, the smaller cations are located closer to the O(2) side of the M(4) site, whereas the larger cations are located nearer the O(5)–O(6) side of the site. These shifts will strongly influence the shape of the M(4) [or M(2) in pyroxene] thermal ellipsoid since each cation species will occupy a slightly different position along the 2-fold axis. Thus, with multiple occupancy the M(4) vibration ellipsoid should increase in magnitude along the 2-fold axis parallel to *b*. If we combine positional disorder with pure thermal vibration (the latter indicated by prolate ellipsoids with the long axes perpendicular to the 2-fold axis), the resulting vibration surface should resemble, or tend toward, an oblate spheroid. This has been observed in several chain silicates. In Figure 11a,b we have plotted the *rms* amplitudes of vibrations for the M(4) and corresponding M(2) cations in selected amphiboles and pyroxenes. In minerals such as tremolite and diopside, where the vibration ellipsoid probably represents almost pure thermal motion, the ellipsoids are highly prolate (Figure 11a) with the long ellipsoid axis perpendicular to the 2-fold axis. In minerals where positional disorder is important (cummingtonite, with Mg, Fe^{2+}, Mn, and Ca in the M(4) site; and pigeonite, with Mg, Ca, and Fe^{2+} in the M(2) site), the ellipsoids are oblate with the short axis almost parallel to the O(4)–M(4)–O(4) in amphiboles or O(2)–M(2)–O(2) in pyroxenes (Figure 11b). In the latter instance, the longest axis corresponds to thermal vibration and the intermediate axis appears to be related to the positional disorder in the M(4) and M(2) sites.

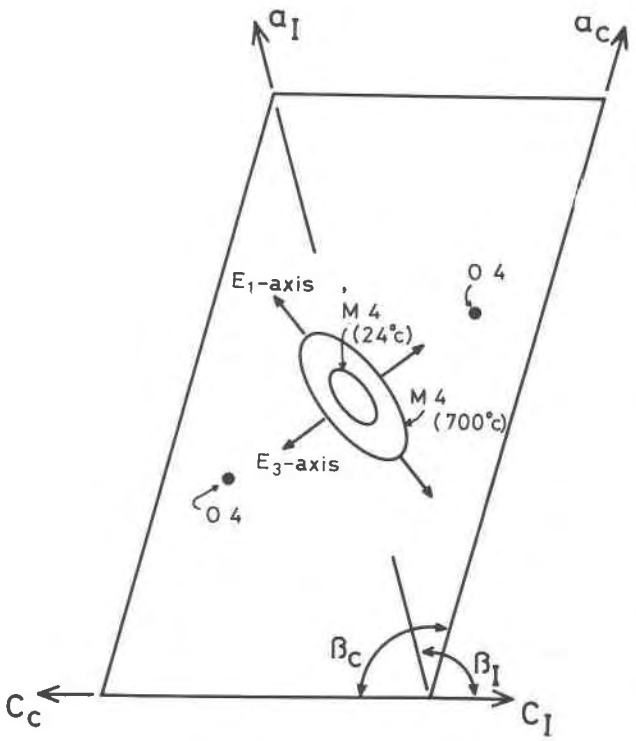

FIG. 10. Diagram of the relative magnitudes and orientations of the thermal ellipsoid of the M(4) cation in tremolite viewed along the *b* axis. The E_1 axis, which is parallel to *ac* plane and almost perpendicular to the O(4)–M(4)–O(4) bonds, is the longest principal axis of the thermal ellipsoid. The E_3 axis, which is parallel to the *ac* plane and almost parallel to the O(4)–M(4)–O(4) bonds, is the shortest one. The E_2 axis is perpendicular to the *ac* plane. The size of the ellipsoids at 24°C and 700°C are exaggerated in scale relative to the unit cell shown here.

Discussion

Cell Parameters

Mean thermal expansion coefficients of the unit cell parameters of tremolite decrease in the order $\alpha_a > \alpha_b > \alpha_c$. In the discussion that follows, we have used "a sin β" or $1/a^*$ since it represents the unit repeat across facing double chains and is equivalent in both the $C2/m$ and $I2/m$ cells. Expansion in the a^* direction is influenced by expansion of the four M-polyhedra and the A site. The value for the mean thermal expansion coefficient of the a sin β is 1.320 $\times$ 10^{-5}/°C (Table 9) which is lower than that expected from a consideration of the values for the A site (α = 3.025 $\times$ 10^{-5}/°C) and the octahedral

layer ($\alpha = 2.172 \times 10^{-5}/°C$)[5] in this direction. However, it must be recalled that a "path" through the structure in the a^* direction includes both octahedral and tetrahedral layers. Since the tetrahedra do not expand, they act as an inert layer, thus effectively reducing the magnitude of $\alpha_a \sin \beta$ for the unit cell.

Expansion along the c crystallographic direction is controlled in large part by the straightening of chains composed of the relatively inert silica tetrahedra. The relatively small amount of chain straightening, an increase in O(5)–O(6)–O(5) of 2.8° over a 700° temperature interval, coupled with the negligible increase in the size of the silicate tetrahedra, exerts a considerable "clamping" or "restraining" effect on expansion along c of the octahedra to which the chains are connected.

The β angle for the C-centered cell of tremolite decreases with increasing temperature (Fig. 2d). This relationship, observed for thermal expansion, contrasts with that found by Whittaker (1960) and Colville *et al* (1966) for chemical expansion, in which larger β_c angles, or smaller β_I angles, could be correlated with larger ionic radii of cations in the $M(4)$ site. Our results for tremolite are consistent with those obtained for cummingtonite (Sueno *et al*, 1972) and for the calcic pyroxenes diopside and hedenbergite (Cameron *et al*, 1973). In Figure 12 we have plotted β_c against a coordination coefficient obtained by dividing the mean $M(4)$–O distance [8-coordinated $M(4)$ cation] by the mean distance for the six shortest $M(4)$–O bonds. Larger coordination coefficients correspond to $M(4)$ cations which are more 6-coordinated, whereas the smaller coefficients correspond to 8-coordinated $M(4)$ cations.

Tetrahedral Chain Displacement

We have also calculated the tetrahedral displacement d, or the distance between the centers of the two opposing six-membered tetrahedral rings ($\equiv$ a − a′ in Figure 13) for different room-temperature amphibole structures and for tremolite structures at different temperatures (Table 13). The centers of each ring are determined by dividing the sum of the z components, projected onto the bc plane, for the six oxygens in each ring by six. (The y components of the oxygen atoms are symmetry related, and therefore the center of the tetrahedral rings must lie within the mirror plane.) This tetrahedral chain displacement is correlated with structural parameters such as (1) the bc projection of the O(5)–O(6)–O(5) angle, (2) the distortion of the silicate tetrahedra, and (3) the c axis component of the O(4)–O(4) distance of $M(2)$. Assuming a constant O(4)–O(4) projected distance, straightening of the tetrahedral chains is positively correlated with increasing displacement. Concomitant with the chain straightening is an increase in the $M(4)$–O(5) distance

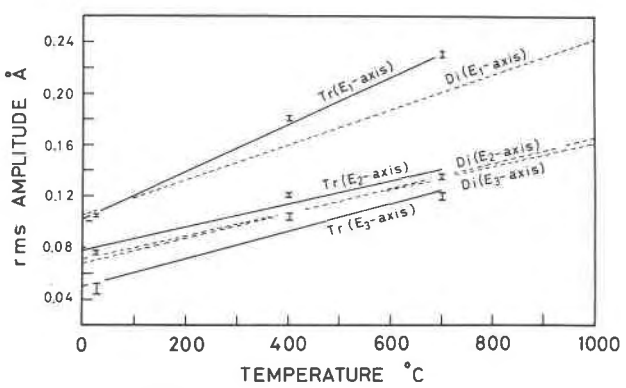

FIG. 11A. Variation of the magnitude of the three principal axes of the thermal ellipsoid of the $M(4)$ cation in tremolite (Tr, solid lines) and the $M(2)$ cation in diopside (Di, broken lines). See text of paper for a detailed explanation of this figure. Error bars represent ±1 standard deviation.

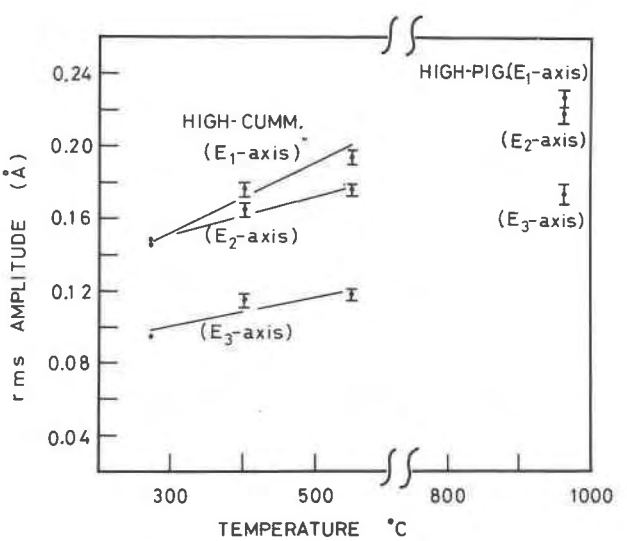

FIG. 11B. Variation of the magnitude of the three principal axes of the thermal ellipsoids of the $M(4)$ cation in cummingtonite (at 270°C, 400°C and 550°C) and the $M(2)$ cation in pigeonite (at 960°C). See text of paper for a detailed explanation of this figure. Error bars represent ±1 standard deviation.

[5] Calculation based on a^* components of O–O distances.

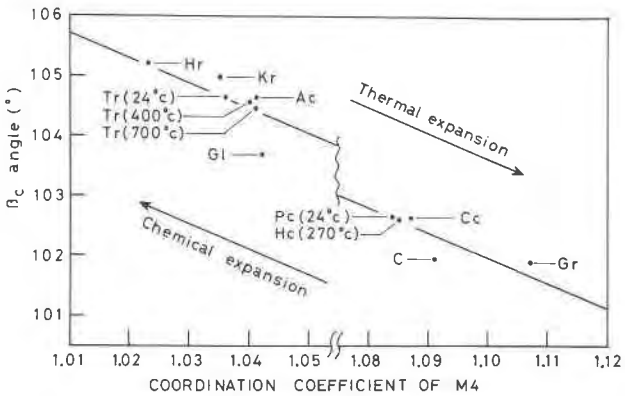

FIG. 12. Diagram of the relationship between the β_c angle and the coordination coefficient

$$\left[= \frac{\text{mean } M(4)\text{–O, if 8-coordinated}}{\text{mean } M(4)\text{–O, if 6-coordinated}}\right]$$

of the $M(4)$ cation. The two arrows indicate the direction of change during thermal expansion and during chemical expansion. Abbreviations: Hr = hornblende, Kr = potassic richterite, Tr = tremolite, Ac = actinolite, Gl = glaucophane, Pc = primitive cummingtonite, Hc = high cummingtonite, Cc = *C*-centered cummingtonite, C = cummingtonite (Ghose, 1961), Gr = grunerite.

which results in the $M(4)$ site becoming more 6-coordinated.

With increasing temperature, the O(5)–O(6)–O(5) angle in tremolite increases and the projection of the O(4)–O(4) distance of the $M(2)$ site onto the *bc* plane slightly decreases. These changes have opposite effects on the chain displacement, the former tending to increase *d*, and the latter to decrease *d*. However, since the tetrahedral chain displacement does increase with increasing temperature, the straightening of the tetrahedral chains appears to be the more important factor in influencing the tetrahedral chain displacement during the thermal expansion of tremolite.

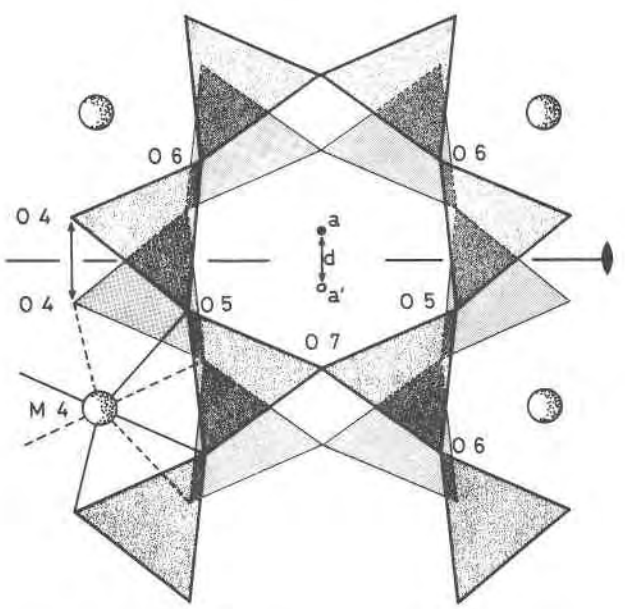

FIG. 13. Diagram of the 6-membered double chains of the tetrahedra in tremolite (24°C) viewed along a^*. (a) and (a') indicate the centers of the upper and lower tetrahedral rings. The length (*d*) is the chain displacement factor in the *bc* plane.

The magnitudes of the displacement factors for most amphiboles fall into two groups (Table 13). Since some of the amphiboles of each group may have similar O(5)–O(6)–O(5) angles, the large displacements of the (Mg,Fe^{2+},Mn) amphiboles can be explained, in part, by the large magnitude of the projection of their O(4)–O(4) distances (1.83–2.01Å) onto the *bc* plane, whereas the small displacement factors of the (Ca,Na) amphiboles can be related to the relatively small projections of their O(4)–O(4) distances (1.40–1.51Å) onto the *bc* plane regardless of their mean $M(2)$–O distances. These significant differences in magnitudes of the projected O(4)–O(4) distances (and chain displacement) reflect the different oxygen configurations about the $M(4)$ cation in the two groups of amphiboles. The relationship between the type of coordination of $M(4)$ and the tetrahedral chain displacement is shown in Figure 14.

Conclusions

1. With increasing temperature, expansion of mean Si–O bonds in both the $T(1)$ and $T(2)$ tetrahedra in tremolite is statistically insignificant.

2. The $M(1)$, $M(2)$, $M(3)$, and $M(4)$ polyhedra exhibit much larger thermal expansions than do the silicate tetrahedra, and mean thermal expansion coefficients for the mean M–O bonds decrease in the order $M(4)$–O > $M(2)$–O > $M(1)$–O > $M(3)$–O. Thermal expansion coefficients for the mean Mg–O and Ca–O bonds in tremolite are similar to those in diopside.

3. Mean thermal expansion coefficients of the volume of the vacant *A* site in tremolite is lower than that of any of the *M*-coordination polyhedra. The site does, however, expand considerably in the a^* direction.

4. The unit cell parameters of tremolite vary linearly as a function of temperature with mean thermal expansion coefficients decreasing as follows: $\alpha_a > \alpha_b > \alpha_c$.

TABLE 13. Coordination Coefficients of $M(4)$, Tetrahedral Chain Displacement Factors, and β_c Angles in Room Temperature and High Temperature Amphibole Structures

	Coordination coefficient of M(4)[a]	Tetrahedral chain displacement factor[a]	β_c angle
Hornblende[b]	1.023	0.1818	105.20
K-richterite[b]	1.035	0.1862	104.98
Tremolite (24°C)[b]	1.036	0.1985	104.65
Tremolite (400°C)[c]	1.040	0.2015	104.57
Tremolite (700°C)[c]	1.041	0.2034	104.46
Actinolite[d]	1.041	0.2041	104.64
Glaucophane[e]	1.042	0.2174	103.67
Primitive-cummingtonite[b]	1.084	0.2710	102.65
High-cummingtonite (270°C)[f]	1.085	0.2724	102.61
C-centered-cummingtonite[b]	1.087	0.2753	102.63
Cummingtonite[g]	1.091	0.2894	101.92
Grunerite[h]	1.107	0.3020	101.88

[a] See text of paper for detailed explanation of these terms.
[b] Refined by Papike, Ross and Clark (1969).
[c] Present study.
[d] Refined by Mitchell, Bloss and Gibbs (1971).
[e] Refined by Papike and Clark (1968).
[f] Refined by Sueno, Papike, Prewitt and Brown (1972).
[g] Refined by Ghose (1961).
[h] Refined by Finger (1969).

5. A positive linear correlation between the coordination coefficient [= mean $M(4)$–O, if 8-coordinated/mean $M(4)$–O, if 6-coordinated] and tetrahedral chain displacement, and a negative correlation between the coordination coefficient and the β_c angle, were found.

6. Rates of increase of equivalent isotropic temperature factors of both the anions and cations can be related to coordination number. For the anions, the 2-coordinated O(7) oxygen has the highest rate of increase and the 4-coordinated O(1) and O(2) oxygens have the lowest rate of increase. For the cations, the temperature factors of the 4-coordinated silicon atoms increase at the lowest rate and that of the 8-coordinated Ca atom increase at the highest rate. Rates of increase for similarly coordinated Mg, Ca, and O atoms in corresponding sites in tremolite and diopside are very similar.

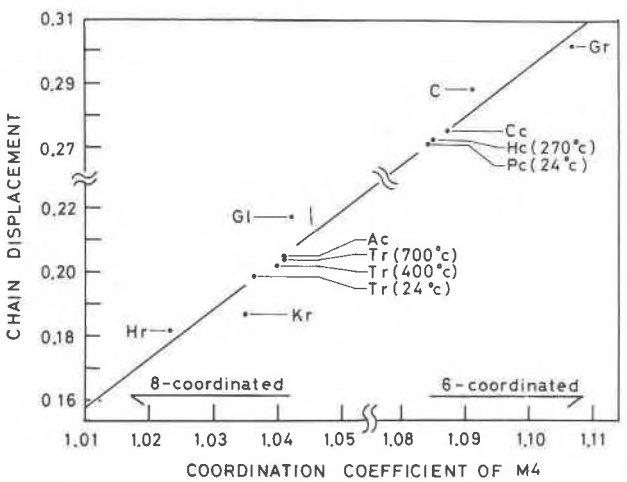

FIG. 14. Diagram of the relationship between the chain displacement factors and the coordination coefficients of $M(4)$ cations in selected amphiboles. (Abbreviations for Figure 12.)

7. When the $M(4)$ site in an amphibole or the $M(2)$ site in a $C2/c$ pyroxene is occupied by several types of atoms, the vibration ellipsoids closely resemble oblate spheroids. The longest ellipsoid axis, perpendicular to the 2-fold axis, corresponds to thermal vibration whereas the second longest axis, parallel to the 2-fold axis, reflects the positional disorder.

8. The similarity of isotropic temperature factors, shape and orientation of thermal ellipsoids, and mean thermal expansion coefficients of mean M–O bonds and polyhedral volumes in tremolite and diopside suggests that it may be possible in some cases to extrapolate thermal expansion data from one mineral group to another.

Acknowledgments

This research was supported by National Science Foundation Grant No. GA-12973.

References

BROWN, G. E., C. T. PREWITT, J. J. PAPIKE, AND S. SUENO (1972) A comparison of the structures of low and high pigeonite. *J. Geophys. Res.* **77,** 5778–5789.

———, S. SUENO, AND C. T. PREWITT (1973) A new single-crystal heater for the precession camera and four-circle diffractometer. *Amer. Mineral.* **58,** 698–704.

CAMERON, M., S. SUENO, C. T. PREWITT, AND J. J. PAPIKE (1973) High-temperature crystal chemistry of acmite, diopside, hedenbergite, jadeite, spodumene, and ureyite. *Amer. Mineral.* **58,** 594–618.

COLVILLE, P. A., W. G. ERNST, AND M. C. GILBERT (1966) Relationships between cell parameters and chemical compositions of monoclinic amphiboles. *Amer. Mineral.* **51,** 1727–1754.

DOYLE, P. A., AND P. A. TURNER (1968) Relativistic Hartree-Fock X-ray and electron scattering factors. *Acta Crystallogr.* **A24,** 390–397.

FINGER, L. W. (1969) The crystal structure and cation distribution of grunerite. *Mineral. Soc. Amer. Spec. Pap.* **2,** 95–100.

GHOSE, S. (1961) The crystal structure of cummingtonite. *Acta Crystallogr.* **14,** 622–627.

MITCHELL, J. T., F. D. BLOSS, AND G. V. GIBBS (1971) Examination of the actinolite structure and four other $C2/m$ amphiboles in term of double bonding. *Z. Kristallogr.* **133,** 273–300.

PAPIKE, J. J., AND JOAN R. CLARK (1968) The crystal structure and cation distribution of glaucophane. *Amer. Mineral.* **53,** 1156–1173.

PAPIKE, J. J., MALCOLM ROSS, AND JOAN R. CLARK (1969) Crystal chemical characterization of clino-amphiboles based on five new structure refinements. *Mineral. Soc. Amer. Spec. Pap.* **2,** 117–136.

SMYTH, J. R. (1971) Protoenstatite: a crystal structure refinement at 1100°C. *Z. Kristallogr.* **134,** 262–274.

———, AND CHARLES W. BURNHAM (1972) The crystal structures of high and low clinohypersthene. *Earth Planet. Sci. Lett.* **14,** 183–189.

SUENO, S., J. J. PAPIKE, C. T. PREWITT, AND G. E. BROWN (1972) The crystal structure of high cummingtonite. *J. Geophys. Res.* **77,** 5767–5777.

TAKEDA, H. (1972) Crystallographic studies of coexisting aluminan orthopyroxene and augite of high-pressure origin. *J. Geophys. Res.* **77,** 5798–5811.

WHITTAKER, E. J. W. (1960) The crystal chemistry of the amphiboles. *Acta Crystallogr.* **13,** 291–298.

ZUSSMAN, J. (1959) A re-examination of the structure of tremolite. *Acta Crystallogr.* **12,** 309–312.

Manuscript received, December 4, 1972;
accepted for publication, February 6, 1973.